Vol. 151: 97–109, 2022
https://doi.org/10.3354/dao03692

DISEASES OF AQUATIC ORGANISMS
Dis Aquat Org

Published online October 13

Wetland cohesion is associated with increased probability of infection by the amphibian chytrid fungus *Batrachochytrium dendrobatidis*

Katherine A. Hulting, Samuel D. Mason, Craig M. Story, Gregory S. Keller*

Landscape Ecology Lab, Department of Life, Health, and Physical Sciences, Gordon College, Wenham, MA 01984, USA

ABSTRACT: The amphibian chytrid fungus *Batrachochytrium dendrobatidis* (*Bd*) poses a substantial threat to amphibian populations. Understanding the landscape conditions that facilitate *Bd* transmission and persistence is crucial for predicting *Bd* trends in amphibian populations. Here, we investigated the interactions between land use, wetland connectivity, and *Bd* occurrence and infection intensity. In northeastern Massachusetts, we sampled *Pseudacris crucifer, Lithobates sylvaticus*, *L. clamitans*, and *L. pipiens* from 24 sites. We found an overall 30.6% *Bd* prevalence at our sites, with prevalence differing among species. *Bd* occurrence increased with wetland-patch cohesion, potentially due to microclimate shifts from decreased forest or changes in host movement. *Bd* infection intensity was not mediated by landscape context. Overall, our results highlight the importance of landscape structure for *Bd* dynamics, suggesting that certain landscapes may facilitate transmission and harbor *Bd* more than others. To mitigate the impacts of *Bd* on amphibian populations, conservation efforts should account for interactions between *Bd* and landscape variables.

KEY WORDS: *Batrachochytrium dendrobatidis* · Amphibian · Frog · Connectivity · Landscape · *Pseudacris* · *Lithobates*

1. INTRODUCTION

Globally, over 40% of amphibian species are in decline and estimated to be threatened with extinction (Gratwicke et al. 2012, IUCN 2021). A major driver of these declines is the emergence of a chytrid fungal pathogen, *Batrachochytrium dendrobatidis* (*Bd*), which causes the disease chytridiomycosis (Berger et al. 1998, Longcore et al. 1999). *Bd* has led to the declines or extinctions of over 500 frog species (Scheele et al. 2019) and poses a serious threat to amphibian biodiversity worldwide (Skerratt et al. 2007, Fisher & Garner 2020). *Bd* was first diagnosed in Australia and Panama (Berger et al. 1998) and infects the keratinized skin of all amphibian orders, disrupting osmotic regulation and depleting electrolytes, resulting in cardiac arrest (Voyles et al. 2009, Wu et al. 2019). The prevalence and infection intensity of *Bd* is affected by many environmental factors; increased *Bd* prevalence and mortality are associated with low temperatures (Kriger & Hero 2007), high elevations (Sapsford et al. 2013), high latitudes (Kriger & Hero 2007), closed canopy (Beyer et al. 2015), greater species richness (Olson et al. 2013), higher precipitation (Longo et al. 2010), higher pH (Kärvemo et al. 2018), and wetland permanence (Beyer et al. 2015).

Recent research has indicated that land cover and habitat structure affect *Bd* transmission and occurrence. Because *Bd* growth and survival are influenced by abiotic factors, changes to surrounding land cover may alter the microclimate to conditions that do not favor *Bd*, such as warmer temperatures with more UV light. For example, Becker & Zamudio

*Corresponding author: greg.keller@gordon.edu

Publisher: Inter-Research · www.int-res.com

(2011) found a negative relationship between habitat loss and *Bd* prevalence and infection intensity in Costa Rica and Australia, and similarly, Saenz et al. (2015) found lower *Bd* occurrence at urban sites compared to forested sites in Texas, USA. Both studies suggested warmer and drier conditions in fragmented areas as causes for reduced *Bd* prevalence. Several studies support that *Bd* prevalence increases with greater extent of natural habitat (Becker et al. 2012, Scheele et al. 2015), although others have found the opposite (Kärvemo et al. 2018), indicating a need for further research in this area.

Because *Bd* is transmitted primarily through motile zoospores in water and direct contact with infected individuals (Berger et al. 2005, Rachowicz & Briggs 2007, Rowley & Alford 2007), areas with higher rates of dispersal and movement may have more disease transmission between populations. Landscapes that facilitate host movement through connectivity are often more susceptible to higher risks of infection (Ostfeld et al. 2005). Sapsford et al. (2013) found that the common mistfrog *Litoria rheocola* had a higher *Bd* prevalence at low-elevation sites that were connected to high-elevation sites compared to noncontiguous low-elevation sites, indicating that aquatic connectivity is a factor in *Bd* transmission. Likewise, proximity to other sites, even without direct aquatic connectivity, may increase *Bd* prevalence. Padgett-Flohr & Hopkins (2010) found that *Bd* occurrence was spatially autocorrelated; sites within 1000–1500 m of known *Bd*-positive sites were more likely to also test *Bd*-positive than isolated sites. Other studies have corroborated these findings (Becker et al. 2017, Costa et al. 2021), indicating that landscape connectivity may alter *Bd* prevalence, with highly connected sites having a higher *Bd* prevalence.

Although connectivity and extent of natural habitat may facilitate the spread of *Bd*, both may be essential for the persistence of frog populations affected by *Bd*. Epidemiological theory for metapopulations proposed by Hess (1996) suggests that for obligate pathogens, the benefits of connectivity are outweighed by the detriments of increased disease transmission, but this hypothesis does not account for patch characteristics (Heard et al. 2015) nor does it necessarily apply to pathogens that can survive without a host for a period of time (Gog et al. 2002). Over 11 yr of monitoring, Heard et al. (2015) found that growling grass frog *L. raniformis* populations declining from *Bd* were sustained through connectivity to patches that did not support *Bd* due to environmental conditions, such as warmer or more saline wetlands. Similarly, Bell et al. (2020) found that upland populations of rainforest frogs in Australia that had previously been extirpated by *Bd* were recolonized when connected to lowland sites that acted as refuges from *Bd*. Because *Bd* is influenced by environmental conditions such as temperature (Sonn et al. 2019, Turner et al. 2021), connectivity between areas with differing environmental conditions (such as upland and lowland sites) may be significant for the persistence of a population, despite increased transmission. However, both Heard et al. (2015) and Bell et al. (2020) focused on connectivity across large elevation gradients, suggesting a need for research on connectivity in areas that do not have this clear gradient of disease risk.

Although *Bd* has been present in the northeastern USA since at least the early 1960s (Ouellet et al. 2005) and models predict that the northeast is highly suitable habitat for *Bd* (Olson et al. 2021), mass die-offs and major species declines due to *Bd* have not been reported in this region. This pattern may be attributed to a lack of long-term monitoring of *Bd* and frog populations in the northeast (Windstam & Olori 2014), or to less pathogenic native strains of *Bd* combined with a degree of resistance in specific northeastern species (Gahl et al. 2012). Previous surveys for *Bd* in the northeastern USA have found occurrences in Connecticut (Richards-Hrdlicka et al. 2013), New York (Windstam & Olori 2014), Massachusetts, Maine, New Hampshire, and Vermont (Longcore et al. 2007). Prevalence is species-specific; in Connecticut, Richards-Hrdlicka et al. (2013) found no *Bd* occurrence in spring peeper *Pseudacris crucifer*, a 14% prevalence in wood frog *Lithobates sylvaticus*, and a 38% prevalence in green frog *L. clamitans* and northern leopard frog *L. pipiens*. The northeastern USA has a relatively high prevalence of *Bd*, but increased monitoring and research in this region is needed to accurately assess the impacts on amphibian populations.

Bd research relies on the accurate detection of *Bd* from environmental samples, most commonly through skin swabs and quantitative polymerase chain reaction (qPCR) (Kriger et al. 2006). This assay has high specificity (few false positives) when proper measures to reduce contamination are taken, but has a higher likelihood of false negatives, leading to an underestimation of *Bd* presence (DiRenzo et al. 2018). Sources of false negatives can include degraded samples or inhibition of the PCR assay, both of which can arise from contaminating environmental material, including microorganisms on field samples (Kriger et al. 2006, Hyatt et al. 2007). Inhibition can be detected by spiking samples with an exogenous internal control (Hyatt et al. 2007) or reduced by

diluting the DNA template (Boyle et al. 2004) or adding a carrier protein such as bovine serum albumin (BSA) (Garland et al. 2010). However, neither of these methods assesses the integrity of the template DNA in the sample. Using host DNA, which should be present in every sample and have the same level of degradation as *Bd* DNA, as an endogenous internal control should provide evidence that the template DNA is not degraded or inhibited through the entire process of sample collection, DNA extraction, and testing with qPCR (Mittelberger et al. 2020). Moreover, such endogenous controls can also be used to normalize the quantification of the template DNA (Mittelberger et al. 2020); for example, the quantity of pathogen target DNA in a sample can be normalized to the endogenous gene to account for sample-to-sample variation. In the commonly used *Bd* assay (Boyle et al. 2004), exogenous controls can be used (Hyatt et al. 2007), but no endogenous gene control is used, which would improve the sensitivity of this analysis by detecting false negatives and removing them from the analysis.

Here, we studied the impacts of land use and connectivity on the infection prevalence and intensity of *Bd* in northeastern Massachusetts. We expected that land use would alter *Bd* occurrence and infection intensity due to microclimate changes and changes in species interactions, which may limit *Bd* survival and transmission. We further expected that highly connected sites would have higher infection intensities due to increased host and zoospore movement. Because changing land use, a loss of connectivity, and *Bd* are all major threats to amphibians, understanding the interaction between these threats is vital for predicting *Bd* dynamics in amphibian populations. Furthermore, we expected *Bd* to be widespread in this region of Massachusetts and its prevalence to vary between our 4 focal species: *P. crucifer, L. pipiens*, *L. sylvaticus*, and *L. clamitans*. Last, we designed an endogenous internal control that amplifies the host DNA of our focal species to ensure *Bd* DNA integrity and normalize *Bd* infection intensity between samples.

2. MATERIALS AND METHODS

2.1. Study sites and site selection

Our study area was in Essex County, Massachusetts, USA, bounded by the UTM coordinates 19T 4722041 N, 342565 E; 4714396 N, 349990 E; 47208 75 N, 364458 E; and 4714762 N, 349986 E. This region is composed of extensive wetlands, deciduous and coniferous forest, agricultural fields, and residential and suburban development (Fig. 1), with elevation ranging from approximately 10–50 m. Average temperature April–May 2021 was 10.1°C, with a maximum of 17.2°C and a minimum of 6.1°C, and total rainfall was 24.5 cm (NOAA 2022).

Wetland habitat comprised approximately 18% of the landscape and included vernal pools, tidal estuaries near the coast (not included in this study), lacustrine wetlands, and palustrine emergent, forested, and scrub-shrub wetlands. Sites were surrounded by forest, with overstory trees including white pine *Pinus strobus*, eastern hemlock *Tsuga canadensis*, oak *Quercus* spp., red maple *Acer rubrum*, American beech *Fagus grandifolia*, birch *Betula* spp., shagbark hickory *Carya ovata*, horse chestnut *Aesculus hippocastanum*, and cherry *Prunus* spp. Understory was composed of seedlings and saplings of overstory trees, in addition to Japanese barberry *Berberis thunbergii*, Japanese honeysuckle *Lonicera japonica*, multiflora rose *Rosa multiflora*, flowering dogwood *Cornus florida*, poison ivy *Toxicodendron radicans*, sassafras *Sassafras albidum*, winterberry *Ilex verticillata*, and viburnum *Viburnum* spp. Common herbaceous species included broadleaf cattail *Typha latifolia*, purple loosestrife *Lythrum salicaria*, jewelweed *Impatiens capensis*, sedges *Carex* spp., broadleaf arrowhead *Sagittaria latifolia*, buttonbush *Cephalanthus occidentalis*, sweet pepperbush *Clethra alnifolia*, and common duckweed *Lemna minor*.

Sites were selected in partnership with a study considering landscape-scale effects on frog population and community trends. Within our study area, we identified 29 sites using the Natural Heritage and Endangered Species Program vernal pool data and the National Wetlands Inventory map (https://www.mass.gov/orgs/massgis-bureau-of-geographic-information). Sites were chosen systematically, focusing on accessible locations and selecting sites with a range of landscape-level characteristics. From these 29 sites, we selected 24 (at least 250 m apart) to sample for *Bd* based on accessibility and the presence of focal species detected by auditory surveys (Fig. 1). We received permission from conservation organizations to sample on their property, or we placed sampling sites in areas accessible to the public.

2.2. *Bd* sampling

To sample for *Bd*, we swabbed individuals of our focal 4 species (*P. crucifer*, *L. pipiens*, *L. sylvaticus*,

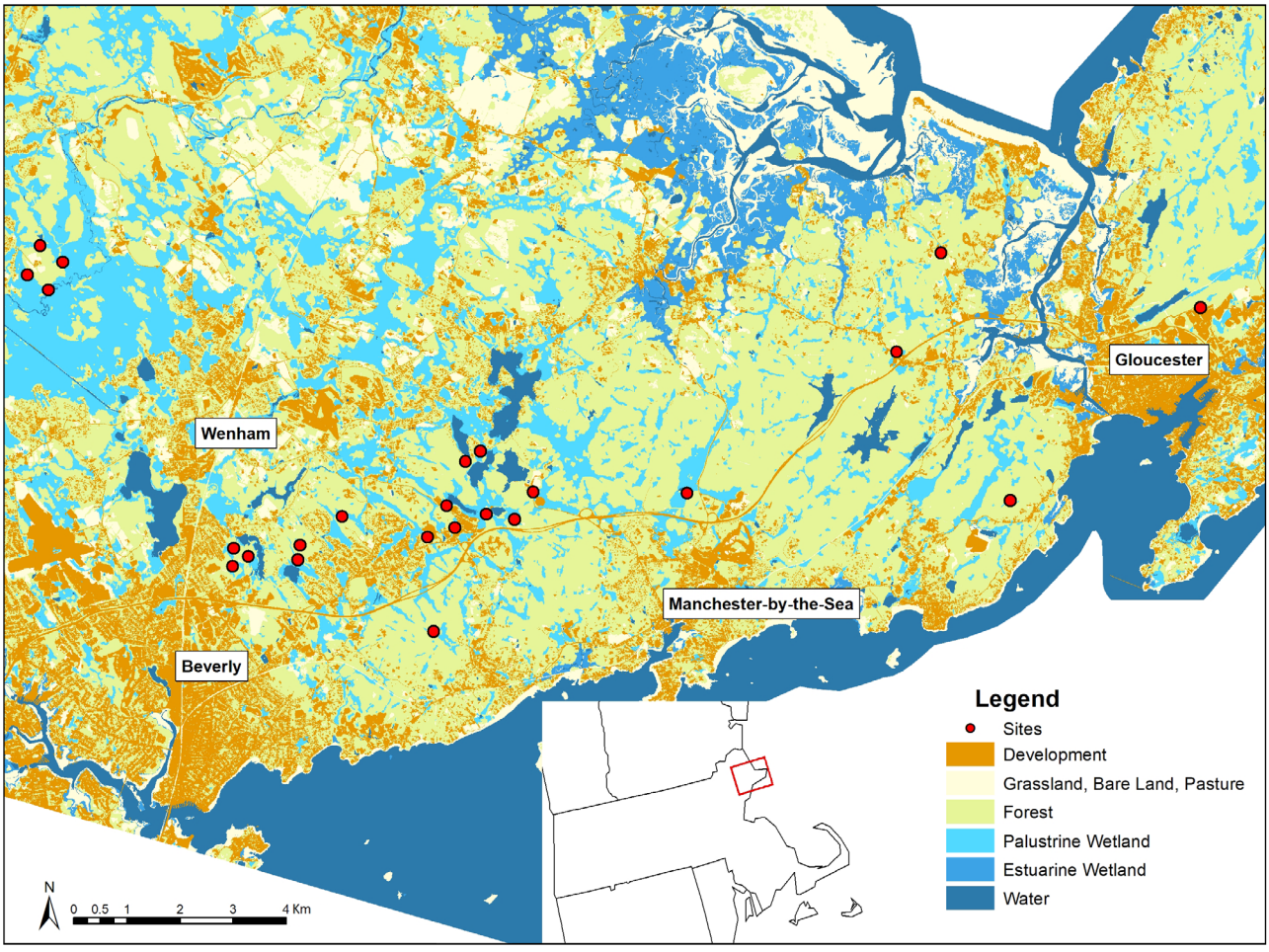

Fig. 1. Land use and locations of 24 study sites surveyed for *Bd* infection in frogs in northeastern Massachusetts, USA

and *L. clamitans*) at these 24 sites between 5 April and 8 May 2021. Each site was visited once to collect samples for an average of 62 min between sunset and 4 h after sunset. Prior to sampling, we recorded air temperature using a regional weather app, estimated cloud cover and wind speed, and recorded whether it had rained within 24 h prior to the survey. Sampling was conducted by an experienced lead researcher and additional trained volunteers.

Focal species were located by sound or sight and captured by hand or a dip net. We handled each individual with a new pair of nitrile gloves to avoid cross-contamination and identified the sex and species of each individual using external characteristics. Using a cotton swab (Puritan® Cotton Tipped Applicator), we swabbed each individual 5 times on either side of the abdomen, inner thigh of each leg, and bottom of each foot, for a total of 30 strokes ind.$^{-1}$ (Hyatt et al. 2007). After swabbing, each individual was kept in a separate plastic bag to avoid repeat sampling, then returned to its original location after sampling at that site was complete. Swabs were stored at −20°C within 2 h of sampling, and all equipment was sterilized using 3% bleach to prevent cross-contamination between sites (Hyatt et al. 2007).

2.3. DNA extraction

To extract DNA from the samples, we added 80 µl of PrepMan Ultra (Applied Biosystems) to each swab and incubated the swab vials for 10 min at 100°C (Hyatt et al. 2007). After cooling for 2 min, we centrifuged the swabs at 19 083 × *g* for 3 min. About 25 µl of extract was transferred to a 1.5 ml Eppendorf tube, then 5 µl of extract was diluted 1:10 in 0.25× TE buffer to minimize PCR inhibition. Extracts were stored at −80°C until testing (Hyatt et al. 2007).

2.4. Primer and probe design

To assess the integrity of our samples and account for potential differences in swabbing pressure and frog body size, we designed an endogenous control to detect the mitochondrial 12S rRNA gene of our 4 focal species (GenBank accession nos. AY843735 [*P. crucifer*], DQ283123 [*L. pipiens*], NC_027236 [*L. sylvaticus*], and DQ283185 [*L. clamitans*]). The 12S rRNA gene sequence is highly conserved among amphibian species, making it a suitable candidate for endogenous control design (Yang et al. 2014). We used BLASTn analysis (https://blast.ncbi.nlm.nih.gov/Blast.cgi) to align the gene sequences of our focal species, then selected locations for a forward primer FrogF (5′-ACA AAC TGG GAT TAG ATA CCC C-3′) and reverse primer FrogR (5′-TCA ART CCT TTG GGT TTT AAG C-3′) to amplify a 103 bp region of the 12S rRNA gene of our focal species (Fig. 2). Within this amplicon, we developed a HEX-labeled locked nucleic acid probe (5′- /5HEX/ TT+G CT+C GTA RTT +CCC +TGG /3IABkFQ/ -3′) (Fig. 2). We used the primers ITS-1 Chtyr3 (5′-CCT TGA TAT AAT ACA GTG TGC CAT ATG TC-3′) and 5.8S (5′-TCG GTT CTC TAG GCA ACA GTT T-3′) and the FAM-labeled minor groove binding probe Chytr MBG2 (5′-/56-FAM/ CGA GTC GAA CAA AAT /3MBG-NFQ/-3′) to detect the internal transcribed spacer (ITS) 1–5.8S rRNA gene of *Bd* (Boyle et al. 2004). All primers and probes were purchased from Integrated DNA Technologies.

To ensure the endogenous control primers and host DNA amplification did not interfere with *Bd* detection, we performed a parallel set of 5-fold dilutions of our *Bd*-positive control (10^6 to 10^2 ITS copies), one with and one without additional host DNA template added. This host DNA template was from a sample that was previously shown to be negative for *Bd*. Both sets of dilutions contained both primer sets, and the dilutions were compared to ensure the amplification of the host DNA did not interfere with the amplification of *Bd*.

2.5. Real-time qPCR assay

We conducted the duplex real-time qPCR assay using the CFX96 real-time system (Bio-Rad Laboratories). Our 20 µl reaction mixture contained 10 µl of 2× Luna Universal Probe qPCR Master Mix (New England BioLabs), *Bd* primers (ITS-1 Chytr3, and 5.8S) at a concentration of 0.4 µM, *Bd* probe (Chytr

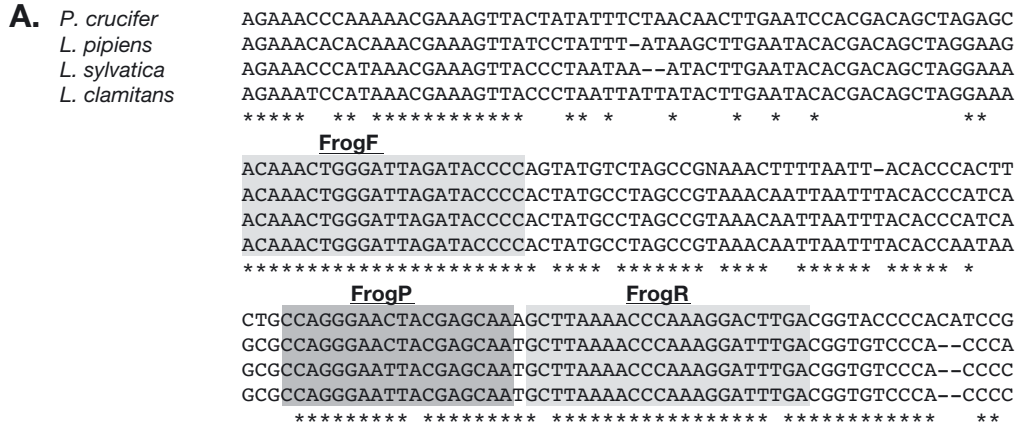

Fig. 2. (A) BLASTn alignment of mitochondrial 12S rRNA gene sequences of *Pseudacris crucifer* (GenBank accession no. AY843735), *Lithobates pipiens* (GenBank accession no. DQ283123), *L. sylvaticus* (GenBank accession no. NC_027236), and *L. clamitans* (GenBank accession no. DQ283185). (B) Primer and probe sequences of the endogenous control. FrogF: forward primer; FrogR: reverse primer; FrogP: probe

MGB2) at a concentration of 0.2 µM, endogenous control primers (FrogF and FrogR) at a concentration of 0.4 µM, endogenous control probe at a concentration of 0.2 µM, 400 ng µl^{-1} BSA, 5 µl of 1:10 diluted DNA template, and 3.4 µl of nuclease-free water (Boyle et al. 2004, Garland et al. 2010). Each sample was prepared in duplicate, along with a duplicate negative control (nuclease-free water) and a 7-fold dilution of *Bd*-positive control DNA (10^7 to 10^1 ITS copies). Our cycling conditions were 95°C for 10 min followed by 40 cycles of 95°C for 15 s and 58°C for 1 min (Blooi et al. 2013). If only one of the duplicate reactions amplified, the sample was retested and considered positive if 2 of the 3 replicates amplified with a quantification cycle [C_q] < 40) (Skerratt et al. 2011). C_q, also known as threshold cycle (C_t), is the first cycle in which the sample signal rises above background (Bustin et al. 2009). Samples where the endogenous control did not amplify were considered degraded and were excluded from the analysis. Two samples that had initially tested positive in the process of designing the endogenous control were also excluded from analysis due to a loss of the *Bd* signal after multiple freeze–thaw cycles.

We normalized *Bd* quantity (i.e. *Bd* intensity) relative to the endogenous control using the $2^{-\Delta\Delta Cq}$ method (Livak & Schmittgen 2001) to adjust for differences in sample collection due to frog body size and swab pressure. The first ΔC_q is the difference between the target gene and the control gene and the $\Delta\Delta C_q$ is the difference between ΔC_q and a calibrator. We chose to use the sample with the highest ΔC_q (lowest *Bd* quantity relative to the endogenous control) as the calibrator. Because this method requires that the primer efficiencies are approximately equal, we compared primer efficiencies using a standard curve. Our primer efficiencies were within 3% (ITS-1 Chtyr3 and 5.8S = 98.68%; FrogF and FrogR = 101.61%). We log transformed our final $2^{-\Delta\Delta Cq}$ values prior to statistical analysis.

2.6. Landscape analysis

Using ArcGIS 10.4.1 (ESRI) and FRAGSTATS 4.2.1 (McGarigal et al. 2012), we quantified connectivity and land use surrounding our sites. We chose to measure 3 land-use metrics and 1 wetland connectivity metric within a 500 m radius of each site, a spatial scale at which frogs frequently respond (Price et al. 2005, Eigenbrod et al. 2008, Simon et al. 2009). Our land-use metrics were (1) forested area (deciduous, coniferous, mixed), (2) developed land area (i.e. residential, suburban, and urban), and (3) paved road density. Our connectivity metric was wetland-patch cohesion. Wetland in this study included vernal pools and palustrine and lacustrine wetlands.

We used 2016 Land Cover/Land Use data to measure land cover surrounding our sites (https://www.mass.gov/info-details/massgis-data-2016-land-cover land-use). This vector data layer was developed from 1 m^2 2016 raster land cover classification and is the most recent land cover classification available for our study area. Land cover surrounding our sites was visually assessed to ensure accuracy. Because some small wetland patches were not delineated as wetland in the 2016 Land Cover/Land Use layer, we manually edited this layer to accurately reflect these patches based on site visits. We summed forested area and developed land area within a 500 m radius of our sites. Paved road density within 500 m was quantified using the linear road length from the 2021 TIGER/Line Shapefile downloaded from the US Census Bureau website (https://www.census.gov/geographies/mapping-files/time-series/geo/tiger-line-file.html).

We used FRAGSTATS to calculate wetland-patch cohesion, which measures the physical aggregation of wetland at the landscape scale. The patch cohesion equation is:

$$\text{COHESION} = \left[1 - \frac{\sum_{j=1}^{n} p_{ij}}{\sum_{j=1}^{n} p_{ij}\sqrt{a_{ij}}}\right]\left[1 - \frac{1}{\sqrt{A}}\right]^{-1} \times 100\% \quad (1)$$

where p_{ij} is the perimeter of the patch *ij* in the focal class (wetland), a_{ij} is the area of the patch *ij*, and A is the total number of cells in the landscape (McGarigal et al. 2012). We used the patch cohesion index as a measure of connectivity because previous research has found that this metric is correlated with dispersal success in simulated models (Schumaker 1996, Tischendorf 2001).

2.7. Statistical analysis

We understood our response variable to be generated by 2 separate biological processes. In order for *Bd* intensity to be quantified (non-zero), the individual must first have been infected. We modeled this system using a gamma hurdle probability framework as defined below:

$$f(y;\alpha,\beta) = \begin{cases} g_{\text{binominal}}(y=0;\alpha), & \text{when } y=0 \\ 1 - g_{\text{binominal}}(y=0;\alpha) \times \dfrac{h_{\text{gamma}}(y;\beta)}{1 - H_{\text{gamma}}(y=0;\beta)}, & \text{when } y>0 \end{cases} \quad (2)$$

When our response variable, *y*, is zero (no *Bd* detected) the conditional probability of *y* is equal to

$g_{\text{binominal}}(y = 0; \alpha)$, where $g_{\text{binominal}}()$ is the binomial probability mass function and α is a vector of logit-linked regression parameters that predicts π, the probability of observing $y = 0$. Once infected with *Bd*, $y > 0$, and the conditional probability of y is equal to the joint probability of $1 - \pi$ and the zero-truncated gamma probability where β is a vector of log-linked regression parameters. Note that $h_{\text{gamma}()}$ is the probability density function and $H_{\text{gamma}()}$ is the cumulative distribution function.

Using this framework, we fit a single hierarchical model to evaluate the relative effects of road density, developed area, and wetland cohesion on *Bd* infection. We included a random site intercept in both model processes to accommodate baseline differences in infection among sites. Wetland cohesion and forest area, another predictor of interest, were linearly correlated (Pearson's r = −0.71). To mitigate the inferential complexities associated with multicollinearity, we did not include forest area in the model (Graham 2003, Harrison et al. 2018). We reasoned that the cohesion variable, which increases as wetland patches in the surrounding landscape become larger and more aggregated, is more ecologically relevant to the life histories of both frogs and *Bd*. Simulated quantile residuals (Hartig 2021) plotted against forest area showed little evidence of model misspecification in the absence of this predictor. Because *Bd* infection may be affected by differences in physiology and habitat use among species, we interacted all landscape predictors with species in both processes of our model. Only *P. crucifer* and *L. clamitans* infection were analyzed due to small sample size for our other focal species.

We fit our model using the 'brm' function from the R package 'brms' v.2.16.3 (Bürkner 2021). We used default uninformative priors on all model parameters. The model was run on 4 chains, each with 5000 iterations where 2500 iterations were burn-in iterations. All chains converged with 0.99 < Rhat < 1.01 and posterior draws were combined. We visually inspected the suitability of our model by comparing the observed distribution of y with 10 y vectors generated from the posterior distribution. All analysis and visualization was completed in R v.4.1.1 (R Core Team 2021).

3. RESULTS

In total, we detected *Bd* at 17 of our 24 sites (70.8%). Of 187 skin swabs from our 4 focal species combined, 30.6% tested positive for *Bd*. *Pseudacris crucifer* was the most commonly sampled species, with 35 of 146 individuals testing positive (24.0%). *Lithobates clamitans* had a higher infection prevalence, with 15 of 29 individuals testing positive (51.7%) (Table 1). *L. sylvaticus* (4 out of 8 positive) and *L. pipiens* (3 out of 3 positive) did not have large enough sample sizes to include in analyses.

3.1. *Bd* occurrence and infection intensity

Bd occurrence, defined as the probability of an individual frog testing positive, varied with wetland cohesion. We found evidence that *Bd* occurrence in *L. clamitans* increased with wetland cohesion, whereas wetland cohesion did not covary with *Bd* occurrence in *P. crucifer* (Fig. 3, Table 2). Evidence for directional associations between occurrence and

Table 1. *Batrachochytrium dentrobatidis* (*Bd*) infection results from skin swabs sampled from frogs in northeastern Massachusetts in April–May 2021. Internal transcribed spacer (ITS) copy number is unadjusted for the endogenous control, and *Bd* intensity is adjusted for the endogenous control using the $2^{-\Delta\Delta Cq}$ method (Livak & Schmittgen 2001)

Species	Sex	Prevalence infected/total (%)	ITS copy median (range)	*Bd* intensity median (range)
Pseudacris crucifer	Male	34/138 (24.6%)	834 (7–91682)	4.46 (0.60–8.96)
	Female	1/8 (12.5%)	16	0.89
Lithobates clamitans	Male	2/4 (50.0%)	784 (47–1521)	2.94 (1.89–3.99)
	Female	13/25 (52.0%)	2951 (140–538935)	3.91 (<0.00–5.87)
Lithobates sylvaticus	Male	3/5 (60.0%)	3249 (161–8379)	5.99 (1.02–6.16)
	Female	1/3 (33.3%)	41062	7.91
Lithobates pipiens	Male	2/2 (100.0%)	68627 (1196–136058)	4.14 (2.74–5.54)
	Female	1/1 (100.0%)	50107	3.66
Total		57/186 (30.6%)	1335 (7–538935)	4.16 (<0.00–9.96)

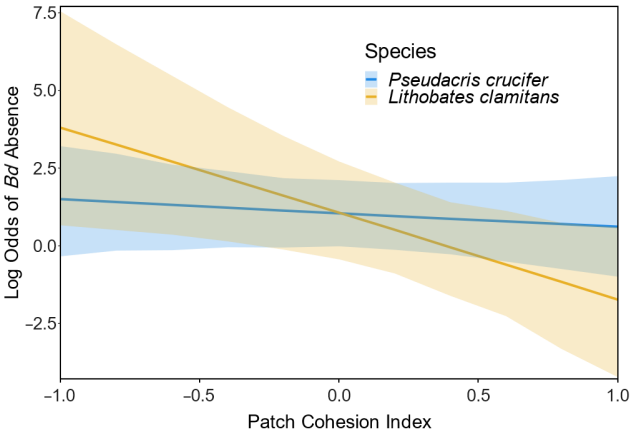

Fig. 3. Log odds of *Batrachochytrium dentrobatidis* (*Bd*) infection absence at sites differing in patch cohesion of wetland (scaled and centered) within a 500 m radius in northeastern Massachusetts. Shaded regions: 90% Bayesian credible intervals

all other landscape variables was low. *Bd* infection intensity, defined as the infection load of an individual frog, was not associated with any land-use or connectivity metrics. The estimated standard deviation of the site-level random slope for the binomial processes was more than double the intercept for either species, indicating high variability in the log-odds of *Bd* occurrence among study sites that is not attributable to species differences or the variation in our landscape predictors (Table 2). By contrast, log *Bd* intensity did not vary as much among sites.

3.2. Endogenous control

Our endogenous control primers and probe successfully amplified and detected DNA from all 4 focal species. The serial dilution of the *Bd* ITS copies amplified consistently with the serial dilution where both the *Bd* ITS copies and endogenous control were amplified, although the highest dilution did not amplify *Bd* (Fig. 4). This result indicates that amplification of the endogenous control did not interfere with the amplification of *Bd* except at the lowest infection intensities of *Bd*. The endogenous control amplified in all samples except one *P. crucifer* sample.

4. DISCUSSION

Our survey indicated that *Bd* infection is widespread in northeastern Massachusetts. Surveys for *Bd* in local amphibian populations in the northeastern USA are lacking (Windstam & Olori 2014), and to our knowledge, this is the first survey of *Bd* in northeastern Massachusetts (Olson et al. 2021). The overall 30.6% *Bd*-positivity prevalence detected in our

Table 2. Hurdle model summary for the effects of land use on *Batrachochytrium dendrobatidis* (*Bd*) absence and intensity, including the mean (estimate), standard deviation (est. error), and 90% Bayesian credible intervals (CI). **Bold** indicates evidence for directional estimates. Full model formula used for both components of the hurdle model was ~ (1|Site) + Species × Road Density + Species × Developed Area + Species × Wetland Cohesion

	Parameter	Estimate	Est. error	90% CI
Bd absence	sd(site-level random effect)	2.70	0.95	(1.46, 4.49)
	Intercept	1.13	0.98	(−0.36, 2.84)
	Species (*Pseudacris crucifer*)	−0.10	0.96	(−1.76, 1.36)
	Road density	−0.62	1.05	(−2.37, 0.99)
	Wetland cohesion	**−2.90**	**1.00**	**(−5.73, −0.60)**
	Developed area	−0.12	1.06	(−1.84, 1.61)
	Species (*P. crucifer*) × road density	−0.32	0.98	(−1.94, 1.23)
	Species (*P. crucifer*) × wetland cohesion	**2.45**	**1.43**	**(0.37, 5.00)**
	Species (*P. crucifer*) × developed area	0.78	0.92	(−0.60, 2.38)
Bd intensity	sd(site-level random effect)	0.24	0.16	(0.02, 0.53)
	Intercept	1.32	0.23	(0.96, 1.71)
	Species (*P. crucifer*)	0.16	0.26	(−0.28, 0.57)
	Road density	0.09	0.25	(−0.28, 0.52)
	Wetland cohesion	0.14	0.51	(−0.63, 1.03)
	Developed area	−0.09	0.28	(−0.56, 0.36)
	Species (*P. crucifer*) × road density	−0.14	0.28	(−0.62, 0.29)
	Species (*P. crucifer*) × wetland cohesion	−0.23	0.54	(−1.17, 0.61)
	Species (*P. crucifer*) × developed area	0.23	0.31	(−0.27, 0.74)

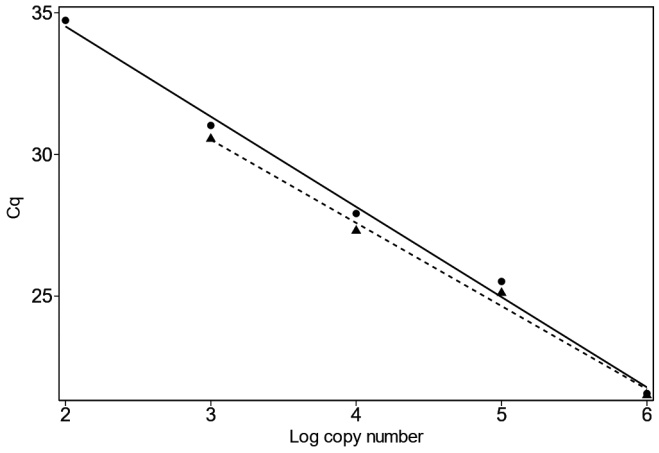

Fig. 4. Comparison between two 5-fold serial dilutions of *Batrachochytrium dentrobatidis* (*Bd*) internal transcribed spacer (ITS) copies. Solid line and points: *Bd* ITS copy amplification without the endogenous control amplified; dashed line and triangles: *Bd* ITS copy amplification with the endogenous control amplified

study area is comparable to other *Bd* surveys in the northeastern USA; for example, Richards-Hrdlicka et al. (2013) found a 28% infection prevalence in Connecticut during May–November, and Windstam & Olori (2014) found a 30% infection prevalence in New York State during April–November. Despite this high prevalence of *Bd*, we did not observe any clinical signs of infection in any sampled individual, suggesting that these populations may have some degree of resistance or tolerance to *Bd* (Gahl et al. 2012, Robinson et al. 2018). Because of this lack of clinical infection, further research is needed to evaluate seasonal chytridiomycosis incidence in this region and identify the rate of positivity relative to the rate of clinical infection and mortality.

4.1. *Bd* occurrence and infection intensity

The spatial distribution of *Bd* occurrence was affected by wetland-patch cohesion. Greater wetland cohesion was associated with higher *Bd* occurrence in *Lithobates clamitans*, with little effect on *Bd* occurrence in *Pseudacris crucifer.* The aggregation of wetlands in a landscape measured by the patch cohesion index may increase *Bd* occurrence through physical connectedness of the wetlands, providing an opportunity for host and zoospore movement. Sapsford et al. (2013) found that aquatic connectivity increased infection prevalence in Australia, indicating zoospore movement between sites as a potential mechanism for this increased infection. Similarly, Padgett-Flohr & Hopkins (2010) found that ponds within 1000–1500 m of a *Bd* hotspot had a higher probability of also testing positive in central California. An increased aggregation of wetland area may increase the chances of physical or functional connection to other *Bd*-infected sites. Infection in *L. clamitans* may be more influenced by wetland aggregation than *P. crucifer*; given the extensive dispersal distances of *L. clamitans* (Schroeder 1976), they may potentially transmit *Bd* between breeding sites at a higher rate.

In our study area, where wetland and forest area are the 2 dominant cover types surrounding our study sites, a high wetland cohesion necessitates decreased forest area (Pearson's r = −0.71), confounding these 2 variables. We might therefore consider that the observed association between cohesion and *Bd* occurrence could be driven, in part, by the ecological implications of reduced forest area in addition to the connectivity considerations discussed above. This potential forest effect contrasts other studies that found that an increased forest area resulted in higher *Bd* occurrence, suggesting the cooler microclimate provided by forest area as an explanation (Pauza et al. 2010, Becker & Zamudio 2011, Saenz et al. 2015, Scheele et al. 2015). These studies, however, were sampling in regions with warmer average spring temperatures than our study area (e.g. Texas, California). The optimal temperature range for *Bd* growth is 17–25°C (Piotrowski et al. 2004). So although the cooler microclimate provided by increased forest area may lower the temperature in warmer climates into this optimal range, it may reduce the temperature below the optimal range in cooler climates (Kärvemo et al. 2018). Although our analysis cannot resolve the effects of wetland connectivity and forest area, we suggest that both should be considered as reasonable explanations for the observed relationship between wetland cohesion and *Bd* occurrence in *L. clamitans*.

Bd occurrence was associated with landscape variables, but patterns in infection intensity were not. We expected the effect of landscape context to be similar in both processes of infection occurrence and intensity because of previous research that has found that natural land cover and connectivity drive infection intensity (Becker & Zamudio 2011, Sapsford et al. 2013). However, these studies found landscape effects on *Bd* intensity when accounting for other factors like elevation or weather, suggesting that in our study, where we did not model these factors, landscape associations may have been missed. Additionally, although land use and connectivity may

impact whether *Bd* is transmitted to or persists at a site, other factors, such as skin microbiome (Woodhams et al. 2007), may have a stronger control on infection intensity.

Infection prevalence varied widely between species. The most commonly sampled species, *P. crucifer*, had a lower infection prevalence (24%) than other species. This *P. crucifer* infection prevalence, however, is higher than previous surveys in the northeastern USA have detected, with many finding no infection in *P. crucifer* (Longcore et al. 2007, Richards-Hrdlicka et al. 2013). In contrast, *L. clamitans*, *L. sylvaticus*, and *L. pipiens* all had a higher *Bd* infection prevalence (Table 1). A high infection prevalence in *L. clamitans* and *L. pipiens* is a common trend in past *Bd* surveys; both species have been identified as potential *Bd* reservoirs (Woodhams et al. 2008, Gahl et al. 2012). Infection prevalence in *L. sylvaticus* is typically lower than detected in our survey (Longcore et al. 2007), although both *L. sylvaticus* and *L. pipiens* results should be interpreted with caution because of small sample sizes.

These differences in infection prevalence between species may be attributed to differences in habitat use. *P. crucifer* is a more terrestrial species, using water primarily for breeding, which may reduce the amount of contact that this species has with *Bd*-contaminated water (Longcore et al. 2007). In contrast, *L. clamitans* and *L. pipiens* are both more aquatic species, spending more time in water that may be *Bd*-contaminated. Lips et al. (2003) found that species in Central America that were more dependent on aquatic habitat experienced the greatest *Bd*-related declines, suggesting that habitat use and contact with water may be important for explaining species differences in infection prevalence.

4.2. Endogenous control

Our endogenous control successfully amplified host DNA from all 4 of our focal species. Because this control was designed from the mitochondrial 12S rRNA gene sequence, which is highly conserved among amphibian species (Yang et al. 2014), it has potential for use beyond our focal species. However, because the control slightly interfered with *Bd* detection (Fig. 4), low *Bd* loads may be missed, suggesting the need for further optimization of this control.

Bd research relies on accurate detection of both infection occurrence and intensity; however, in the commonly used *Bd* assay, there is no method to assess the integrity of the DNA template. Our endogenous control design provides confidence that the samples used in our analysis were not degraded or inhibited at any stage in *Bd* detection and lowers the chance of false negatives. Although only one of our samples was excluded as a false negative, *Bd* sampling in remote regions with less optimal sample collection and storage conditions may have higher rates of false negatives (Van Sluys et al. 2008). DiRenzo et al. (2018) estimated that *Bd* prevalence is underestimated by up to 71% due to false negatives, supporting the importance of an endogenous control.

Another advantage of including an endogenous control is that it may be used to normalize infection intensity between samples. *Bd* quantity sampled by a swab may vary with differences in swabbing technique or pressure (Retallick et al. 2006), and because there is no standardized swabbing technique in *Bd* research (Richards-Hrdlicka et al. 2013), infection intensity comparison between studies may be inconsistent. Furthermore, differences in body size between individuals may also skew infection intensity detection unless *Bd* quantity is normalized against host DNA. This normalization, however, assumes that the quantity of *Bd* and the endogenous control vary proportionally with swab pressure and frog size, which requires further testing to confirm. Additionally, individuals with high infection loads often experience a higher rate of skin sloughing (Ohmer et al. 2015), which may also affect the quantity of the endogenous control. Nevertheless, the universal use of an endogenous control in the *Bd* assay would facilitate comparison between studies.

4.3. Conclusions

We detected a high infection prevalence of *Bd* in northeastern Massachusetts, although prevalence varied widely between species. Because of this high prevalence, we recommend long-term monitoring of *Bd* in the northeastern USA to evaluate mortality rates and *Bd*-driven population changes. Additionally, we found that wetland-patch cohesion was associated with *Bd* occurrence in *L. clamitans*, highlighting the potential influence that landscape context has on disease dynamics. Our results indicate that *Bd* risk is non-randomly distributed across a gradient of land use; some land-use compositions may provide suitable environmental conditions for *Bd*, as well as altering host movement and density. Because of the high correlation between forest and wetland-patch cohesion, we recommend further research to disentangle their relative effects on the spatial distribution

of *Bd*. Understanding factors that alter *Bd* occurrence and intensity is critical for evaluating the susceptibility of a population to *Bd* and developing plans to conserve at-risk populations.

Acknowledgements. We thank Gordon College, the Massachusetts Board of Trustees, Mass Audubon Ipswich River Wildlife Sanctuary, Essex County Greenbelt Association, Manchester Essex Conservation Trust, and Manchester-by-the-Sea Conservation Commission for allowing us to sample on their properties. We thank A. Strubberg and K. Stevens of IDT for assistance with probe design, K. Anderson for assistance with qPCR protocols, and B. LaBumbard and the Woodhams Lab for providing *Bd* standards. We also thank D. Boorse for providing comments on drafts of the manuscript. Lastly, we thank M. Anderson, A. Bekas, C. Berry, M. Blouchard, K. Boothby, M. Chan, C. Charek, R. Corbin, J. Kuznicki, D. Leslie, O. Martorelli, R. Muir, E. Mulroy, L. Pacchioli, A. Siebert, A. Thayer, and G. Vienneau for assistance with fieldwork.

LITERATURE CITED

Becker CG, Zamudio KR (2011) Tropical amphibian populations experience higher disease risk in natural habitats. Proc Natl Acad Sci USA 108:9893–9898

Becker CG, Rodriguez D, Longo AV, Talaba AL, Zamudio KR (2012) Disease risk in temperate amphibian populations is higher at closed-canopy sites. PLOS ONE 7: e48205

Becker CG, Longo AV, Haddad CFB, Zamudio KR (2017) Land cover and forest connectivity alter the interactions among host, pathogen and skin microbiome. Proc R Soc B 284:e20170582

Bell SC, Heard GW, Berger L, Skerratt LF (2020) Connectivity over a disease risk gradient enables recovery of rainforest frogs. Ecol Appl 30:e02152

Berger L, Speare R, Daszak P, Green DE and others (1998) Chytridiomycosis causes amphibian mortality associated with population declines in the rain forests of Australia and Central America. Proc Natl Acad Sci USA 95:9031–9036

Berger L, Hyatt AD, Speare R, Longcore JE (2005) Life cycle stages of the amphibian chytrid *Batrachochytrium dendrobatidis.* Dis Aquat Org 68:51–63

Beyer SE, Phillips CA, Schooley RL (2015) Canopy cover and drought influence the landscape epidemiology of an amphibian chytrid fungus. Ecosphere 6:art78

Blooi M, Longcore JE, Spitzen-van der Sluijs A, Vercammen F, Martel A (2013) Duplex real-time PCR for rapid simultaneous detection of *Batrachochytrium dendrobatidis* and *Batrachochytrium salamandrivorans* in amphibian samples. J Clin Microbiol 51:4173–4177

Boyle DG, Boyle DB, Olsen V, Morgan JAT, Hyatt AD (2004) Rapid quantitative detection of chytridiomycosis (*Batrachochytrium dendrobatidis*) in amphibian samples using real-time Taqman PCR assay. Dis Aquat Org 60:141–148

Bürkner P (2021) brms: an R package for Bayesian multilevel models using Stan. J Stat Softw 100(5):1–54

Bustin SA, Benes V, Garson JA, Hellemans J and others (2009) The MIQE guidelines: minimum information for publication of quantitative real-time PCR experiments. Clin Chem 55:611–622

Costa A, Dondero L, Allaria G, Sanchez BNM, Rosa G, Salvidio S, Grasselli E (2021) Modelling the amphibian chytrid fungus spread by connectivity analysis: towards a national monitoring network in Italy. Biodivers Conserv 30:2807–2825

DiRenzo GV, Grant EHC, Longo AV, Che-Castaldo C, Zamudio KR, Lips KR (2018) Imperfect pathogen detection from non-invasive skin swabs biases disease inference. Methods Ecol Evol 9:380–389

Eigenbrod F, Hecnar SJ, Fahrig L (2008) The relative effects of road traffic and forest cover on anuran populations. Biol Conserv 141:35–46

Fisher MC, Garner TWJ (2020) Chytrid fungi and global amphibian declines. Nat Rev Microbiol 18:332–343

Gahl MK, Longcore JE, Houlahan JE (2012) Varying responses of northeastern North American amphibians to the chytrid pathogen *Batrachochytrium dendrobatidis.* Conserv Biol 26:135–141

Garland S, Baker A, Phillott AD, Skerratt LF (2010) BSA reduced inhibition in a TaqMan® assay for the detection of *Batrachochytrium dendrobatidis.* Dis Aquat Org 92: 113–116

Gog J, Woodroffe R, Swinton J (2002) Disease in endangered metapopulations: the importance of alternative hosts. Proc R Soc B 269:671–676

Graham MH (2003) Confronting multicollinearity in ecological multiple regression. Ecology 84:2809–2815

Gratwicke B, Lovejoy TE, Wildt DE (2012) Will amphibians croak under the Endangered Species Act? Bioscience 62: 197–202

Harrison XA, Donaldson L, Carrea-Cano ME, Evans J and others (2018) A brief introduction to mixed effects modelling and multi-model inference in ecology. PeerJ 6:e4794

Hartig F (2021) DHARMa: residual diagnostics for hierarchical (multi-level/mixed) regression models. R package version 0.4.4. https://CRAN.R-project.org/package=DHARMa

Heard GW, Thomas CD, Hodgson JA, Scroggie MP, Ramsey DSL, Clemann N (2015) Refugia and connectivity sustain amphibian metapopulations afflicted by disease. Ecol Lett 18:853–863

Hess GR (1996) Linking extinction to connectivity and habitat destruction in metapopulation models. Am Nat 148: 226–236

Hyatt AD, Boyle DG, Olsen V, Boyle DB and others (2007) Diagnostic assays and sampling protocols for the detection of *Batrachochytrium dendrobatidis.* Dis Aquat Org 73:175–192

IUCN (2021) The IUCN Red List of Threatened Species, version 2021-3. https://www.iucnredlist.org (accessed 5 July 2022)

Kärvemo S, Meurling S, Berger D, Höglund J, Laurila A (2018) Effects of host species and environmental factors on the prevalence of *Batrachochytrium dendrobatidis* in northern Europe. PLOS ONE 13:e0199852

Kriger KM, Hero JM (2007) Large-scale seasonal variation in the prevalence and severity of chytridiomycosis. J Zool 271:352–359

Kriger KM, Hines HB, Hyatt AD, Boyle DG, Hero JM (2006) Techniques for detecting chytridiomycosis in wild frogs: comparing histology with real-time TaqMan PCR. Dis Aquat Org 71:141–148

Lips KR, Reeve JD, Witters LR (2003) Ecological traits predicting amphibian population declines in Central America. Conserv Biol 17:1078–1088

Livak KJ, Schmittgen TD (2001) Analysis of relative gene expression data using real-time quantitative PCR and the $2^{-\Delta\Delta CT}$ method. Methods 25:402–408

Longcore JE, Pessier AP, Nichols DK (1999) *Batrachochytrium dendrobatidis* gen. et sp. nov., a chytrid pathogenic to amphibians. Mycologia 91:219–227

Longcore JR, Longcore JE, Pessier AP, Halteman WA (2007) Chytridiomycosis widespread in anurans of northeastern United States. J Wildl Manag 71:435–444

Longo AV, Burrows PA, Joglar RL (2010) Seasonality of *Batrachochytrium dendrobatidis* infection in direct-developing frogs suggests a mechanism for persistence. Dis Aquat Org 92:253–260

McGarigal K, Cushman SA, Ene E (2012) FRAGSTATS v4: spatial pattern analysis program for categorical and continuous maps. Tech Rep, University of Massachusetts, Amherst, MA

Mittelberger C, Obkircher L, Oberkofler V, Ianeselli A and others (2020) Development of a universal endogenous qPCR control for eukaryotic DNA samples. Plant Methods 16:53

NOAA (2022) Climate at a glance: global mapping. https://www.ncei.noaa.gov/cag/ (accessed 6 July 2022)

Ohmer MEB, Cramp RL, White CR, Franklin CE (2015) Skin sloughing rate increases with chytrid fungus infection load in a susceptible amphibian. Funct Ecol 29:674–682

Olson DH, Ronnenberg KL, Glidden CK, Christiansen KR, Blaustein AR (2021) Global patterns of the fungal pathogen *Batrachochytrium dendrobatidis* support conservation urgency. Front Vet Sci 8:685877

Olson DH, Aanensen DM, Ronnenberg KL, Powell CI and others (2013) Mapping the global emergence of *Batrachochytrium dendrobatidis*, the amphibian chytrid fungus. PLOS ONE 8:e56802

Ostfeld RS, Glass GE, Keesing F (2005) Spatial epidemiology: an emerging (or re-emerging) discipline. Trends Ecol Evol 20:328–336

Ouellet M, Mikaelian I, Pauli BD, Rodrigue J, Green DM (2005) Historical evidence of widespread chytrid infection in North American amphibian populations. Conserv Biol 19:1431–1440

Padgett-Flohr GE, Hopkins RL (2010) Landscape epidemiology of *Batrachochytrium dendrobatidis* in central California. Ecography 33:688–697

Pauza MD, Driessen MM, Skerratt LF (2010) Distribution and risk factors for spread of amphibian chytrid fungus *Batrachochytrium dendrobatidis* in the Tasmanian Wilderness World Heritage Area, Australia. Dis Aquat Org 92:193–199

Piotrowski JS, Annis SL, Longcore JE (2004) Physiology of *Batrachochytrium dendrobatidis,* a chytrid pathogen of amphibians. Mycologia 96:9–15

Price SJ, Marks DR, Howe RW, Hanowski JM, Niemi GJ (2005) The importance of spatial scale for conservation and assessment of anuran populations in coastal wetlands of the western Great Lakes, USA. Landsc Ecol 20: 441–454

R Core Team (2021) R: a language and environment for statistical computing. R Foundation for Statistical Computing, Vienna

Rachowicz LJ, Briggs CJ (2007) Quantifying the disease transmission function: effects of density on *Batrachochytrium dendrobatidis* transmission in the mountain yellow-legged frog *Rana muscosa.* J Anim Ecol 76: 711–721

Retallick RWR, Miera V, Richards KL, Field KJ, Collins JP (2006) A non-lethal technique for detecting the chytrid fungus *Batrachochytrium dendrobatidis* on tadpoles. Dis Aquat Org 72:77–85

Richards-Hrdlicka KL, Richardson JL, Mohabir L (2013) First survey for the amphibian chytrid fungus *Batrachochytrium dendrobatidis* in Connecticut (USA) finds widespread prevalence. Dis Aquat Org 102:169–180

Robinson CW, McNulty SA, Titus VR (2018) No safe space: prevalence and distribution of *Batrachochytrium dendrobatidis* in amphibians in a highly-protected landscape. Herpetol Conserv Biol 13:373–382

Rowley JJL, Alford RA (2007) Behaviour of Australian rainforest stream frogs may affect the transmission of chytridiomycosis. Dis Aquat Org 77:1–9

Saenz D, Hall TL, Kwiatkowski MA (2015) Effects of urbanization on the occurrence of *Batrachochytrium dendrobatidis*: Do urban environments provide refuge from the amphibian chytrid fungus? Urban Ecosyst 18: 333–340

Sapsford SJ, Alford RA, Schwarzkopf L (2013) Elevation, temperature, and aquatic connectivity all influence the infection dynamics of the amphibian chytrid fungus in adult frogs. PLOS ONE 8:e82425

Scheele BC, Driscoll DA, Fisher J, Fletcher AW, Hanspach J, Vörös J, Hartel T (2015) Landscape context influences chytrid fungus distribution in an endangered European amphibian. Anim Conserv 18:480–488

Scheele BC, Pasmans F, Skerratt LF, Berger L and others (2019) Amphibian fungal panzootic causes catastrophic and ongoing loss of biodiversity. Science 363: 1459–1463

Schroeder EE (1976) Dispersal and movement of newly transformed green frogs, *Rana clamitans.* Am Midl Nat 95:471–474

Schumaker NH (1996) Using landscape indices to predict habitat connectivity. Ecology 77:1210–1225

Simon JA, Snodgrass JW, Casey RE, Sparling DW (2009) Spatial correlates of amphibian use of constructed wetlands in an urban landscape. Landsc Ecol 24:361–373

Skerratt LF, Berger L, Speare R, Cashins S and others (2007) Spread of chytridiomycosis has caused the rapid global decline and extinction of frogs. Ecohealth 4:125–134

Skerratt LF, Mendez D, McDonald KR, Garland S, Livingstone J, Berger L, Speare R (2011) Validation of diagnostic tests in wildlife: the case of chytridiomycosis in wild amphibians. J Herpetol 45:444–450

Sonn JM, Utz RM, Richards-Zawacki CL (2019) Effects of latitudinal, seasonal, and daily temperature variations on chytrid fungal infections in a North American frog. Ecosphere 10:e02892

Tischendorf L (2001) Can landscape indices predict ecological processes consistently? Landsc Ecol 16:235–254

Turner A, Wassens S, Heard G, Peters A (2021) Temperature as a driver of the pathogenicity and virulence of amphibian chytrid fungus *Batrachochytrium dendrobatidis*: a systematic review. J Wildl Dis 57:477–494

Van Sluys M, Kriger KM, Phillott AD, Campbell R, Skerratt LF, Hero JM (2008) Storage of samples at high temperatures reduces the amount of amphibian chytrid fungus *Batrachochytrium dendrobatidis* DNA detectable by PCR assay. Dis Aquat Org 81:93–97

Voyles J, Young S, Berger L, Campbell C and others (2009) Pathogens of chytridiomycosis, a cause of catastrophic amphibian declines. Science 326:582–585

Windstam ST, Olori JC (2014) Proportion of host carrying *Batrachochytrium dendrobatidis*, causal agent of amphibian chytridiomycosis, in Oswego County, NY in 2012. Northeast Nat 21:25–34

Woodhams DC, Vredenburg VT, Simon MA, Billheimer D and others (2007) Symbiotic bacteria contribute to innate immune defenses of the threatened mountain yellow-legged frog, *Rana muscosa*. Biol Conserv 138:390–398

Woodhams DC, Hyatt AD, Boyle DG, Rollins-Smith LA (2008) The northern leopard frog *Rana pipiens* is a widespread reservoir species harboring *Batrachochytrium dendrobatidis* in North America. Herpetol Rev 39:66–68

Wu NC, Cramp RL, Ohmer ME, Franklin CE (2019) Epidermal epidemic: unravelling the pathogenesis of chytridiomycosis. J Exp Biol 222:jeb191817

Yang L, Tan Z, Wang D, Xue L, Guan M, Huang T, Li R (2014) Species identification through mitochondrial rRNA genetic analysis. Sci Rep 4:4089

Editorial responsibility: Douglas Woodhams, Boston, Massachusetts, USA
Reviewed by: B. Inman and 2 anonymous referees

Submitted: May 25, 2022
Accepted: August 2, 2022
Proofs received from author(s): September 30, 2022